Atmos. Chem. Phys., 25, 14629–14642, 2025 https://doi.org/10.5194/acp-25-14629-2025 © Author(s) 2025. This work is distributed under the Creative Commons Attribution 4.0 License.





Composition and Formation Mechanism of Brown Carbon: Identification and Quantification of Phenolic Precursors

Md. Al-Amin Hossen¹, Mehedi Hasan Shakil¹, Md. Fahim Ehasan², Abu Rayhan Mohammad Tareq², and Abdus Salam¹

¹Department of Chemistry, Faculty of Science, University of Dhaka, Dhaka-1000, Bangladesh ²Environmental and Organic Chemistry Laboratory, Chemistry Division, Atomic Energy Centre Dhaka, Bangladesh

Correspondence: Abdus Salam (asalam@gmail.com, asalam@du.ac.bd)

Received: 28 April 2025 – Discussion started: 26 June 2025 Revised: 28 September 2025 – Accepted: 29 September 2025 – Published: 4 November 2025

Abstract. Light-absorbing organic carbon, collectively known as brown carbon (BrC), significantly influences climate and air quality, particularly in urban environments like Dhaka, Bangladesh. Despite their significance, the contributions and transformation pathways of phenolic compounds - major precursors of brown carbon (BrC) – are still insufficiently understood in the South Asian megacities. This study addresses this gap by investigating the surface morphology of PM_{2.5}, quantifying seven phenolic BrC precursors, and exploring the aqueous-phase formation pathway of nitrophenols at two urban sites (Dhaka South and Dhaka North) from July 2023 to January 2024. Phenolic compounds, including phenol, methylphenols, methoxyphenol, hydroxyphenol, and nitrophenol were identified and quantified using gas chromatography-flame ionization detector (GC-FID). PM_{2.5} surface morphology and elemental composition were analyzed via Field Emission Scanning Electron Microscopy – Energy Dispersive X-ray Spectroscopy (FESEM-EDX), and functional groups were characterized using Attenuated Total Reflectance - Fourier Transform Infrared Spectroscopy (ATR-FTIR). Results revealed that PM_{2.5} particles were predominantly spherical or chain-like with carbonaceous elements (C, O, N, S), mineral dust, and trace metals. The dominant functional groups included aromatic conjugate double bond, carbonyl, and nitro group. Aqueous-phase nitration of 2-hydroxyphenol under acidic conditions, analyzed via UV-Vis spectroscopy, demonstrated an alternative nitrophenol formation pathway. Among the detected compounds, 2-hydroxyphenol and 4-nitrophenol showed the highest average concentrations (2.31 ± 1.39 and $2.20 \pm 1.21 \,\mu g \, m^{-3}$, respectively). Seasonal variations showed elevated nitrophenol levels during winter, especially in Dhaka South $(4.54 \pm 2.94 \,\mu g \, m^{-3})$. These findings highlight the quantification of phenolic precursors and the role of aqueous-phase reactions in BrC formation, providing valuable insights for future atmospheric modeling and air quality management strategies in South Asia.

1 Introduction

Brown carbon (BrC) is a type of organic carbon that absorbs light at short wavelengths, such as 300–400 nm (Laskin et al., 2015). In contrast to black carbon, BrC exhibits a wavelength-dependent absorptivity that increases significantly towards the higher energy end of the spectrum (Wang et al., 2023). Similar to black carbon, BrC also has a positive

radiative effect, which lowers the total cooling effect of atmospheric aerosols caused by light scattering (Feng et al., 2013). Because of the complexity and variety of its origins, composition, and atmospheric aging mechanisms, the direct radiative effect of BrC is still unknown despite intensive research (Lee et al., 2014). The two main sources of BrC were vehicle emissions and biomass burning. The composition of primary emissions can differ significantly depending on the type of

fuel and the conditions under which it burns (Laskin et al., 2015). There are probably thousands of organic molecules in atmospheric BrC, many of which are unidentified. However, phenolic compounds are a class of components that are commonly discovered (Wang et al., 2018b). Phenolic and nitrated phenols are organic substances that contain at least one hydroxyl group and a nitro group in the benzene ring. Phenolic derivatives are the major component of BrC. They originate from diverse processes of production and different emission sources. Large volumes of nitrated phenolic compounds are released into the atmosphere by primary sources such as vehicle exhaust, burning of biomass, and combustion of coal (Li et al., 2020; Wang et al., 2020). The secondary synthesis of these substances from precursors like aromatic hydrocarbons and phenolic compounds via nitration in both gaseous or aqueous phases (Harrison et al., 2005).

According to earlier research, one of the main contributors of BrC is nitrated phenolic compounds and R-NO₂ nitroaromatic compounds (Hossen et al., 2023; Li et al., 2022). The main reasons for the increased focus on phenolic compounds are their human toxicity (Rahman et al., 2022) and their role in producing secondary organic aerosols (SOAs) (Nakao et al., 2011). According to previous research, phenol and cresols (such as m-cresol, p-cresol, and o-cresol) can oxidize to produce nitrophenol and its derivatives (Harrison et al., 2005). Cresols released during the burning of biomass can undergo photooxidation, producing nitro-catechol and its derivatives (Finewax et al., 2018; Iinuma et al., 2010). Furthermore, studies conducted by Andreozzi et al. (2006) and Hummel et al. (2010) have demonstrated that the primary pathway for the creation of 3-nitrosalicylic acid and 5-nitrosalicylic acid in the aqueous phase is the nitration of salicylic acid. Laboratory investigations have established the importance of aqueous processes as a production mechanism for nitrated phenolic compounds. In particular, when phenol was subjected to aqueous-phase interactions with nitronium ions (NO_2^+) , 4-nitrophenol was produced (Heal et al., 2007). The most prevalent nitro-aromatic species were nitrophenols and nitro catechols, which accounted for 31 % and 32 % of all nitro-aromatic compounds, respectively (Wang et al., 2021). To fully understand the precursor of BrC in the atmosphere, it is crucial to analyze the concentrations, chemical compositions, and sources of their phenolic precursors, along with the derivatives of nitrated and methyl derivatives of phenols. Aerosol surface morphology plays an important role in the light-absorbing properties and reactivity of BrC. Irregular or porous particle surfaces can enhance the adsorption of gaseous precursors, such as phenolic compounds, thereby influencing their heterogeneous oxidation and nitration pathways in the atmosphere (Liu et al., 2020; Wang et al., 2024). Moreover, morphological features can affect how BrC and its phenolic components interact with cloud or fog droplets, altering aqueous-phase reaction rates and the formation of light-absorbing secondary products.

In Bangladesh, most pollutants originate from vehicle emissions, solid waste burning, biomass burning, and brick kiln emissions (Hossain et al., 2024; Kumar et al., 2021). All these are major sources of BrC. Therefore, studies on BrC composition, such as phenolic compounds and their derivatives, in Bangladesh are essential. In previous studies, Ankhy et al. (2024); Hossen et al. (2023); and Runa et al. (2022) determined the optical properties of BrC emissions from biomass burning as well as ambient air in Dhaka, Bangladesh, but did not investigate the individual composition of BrC. Previous studies have primarily emphasized gasphase reactions between phenolic VOCs and NOx, followed by photochemical oxidation and subsequent partitioning into the particle phase (Hems et al., 2021; Laskin et al., 2015). Yang et al. (2021) reported that photooxidation of phenolic compounds forms BrC, and phenolic compounds are a major class of aromatic compounds known as BrC precursors. Li et al. (2020) show the formation pathway of nitro aromatic compounds via gas-phase reactions, occurring through *OH + NO₂ in daytime and *NO₃+ NO₂ at nighttime. Our study reports an alternative pathway for the formation of nitroaromatic compounds in aqueous-phase reactions through electrophilic substitution (mediated by NO₂⁺ or HONO) under acidic or alkaline conditions in the absence of sunlight, with demonstrated applicability to biomass samples. The main focus of this work, however, is the quantification of phenolic precursors of BrC. Specifically, we investigate the surface composition of PM_{2.5} and phenolic precursors in the atmosphere of Dhaka, Bangladesh, from July 2023 to January 2024, along with an experiment on the aqueous nitration of 2-hydroxyphenol, a common BrC precursor.

2 Methodology

2.1 Sampling sites

PM_{2.5} samples were collected from ambient air at two distinct locations in Dhaka city: Dhaka North (Shah Alibag, Mirpur-1) and Dhaka South (Department of Chemistry, University of Dhaka) (Fig. S1 in the Supplement). Both sampling sites were situated approximately 21 m above the ground level. The Dhaka South site, while located within an educational institution, was adjacent to a busy highway with frequent traffic congestion. Additionally, metro rail construction was ongoing nearby, further contributing to the area's pollution levels. The Dhaka North site, a mixed residential and commercial zone, was surrounded by garment factories, pharmaceutical plants, shopping centers, and restaurants. It was situated about 100 m from the Mirpur bus station and approximately 4 km from the Taltola solid waste dumping yard.

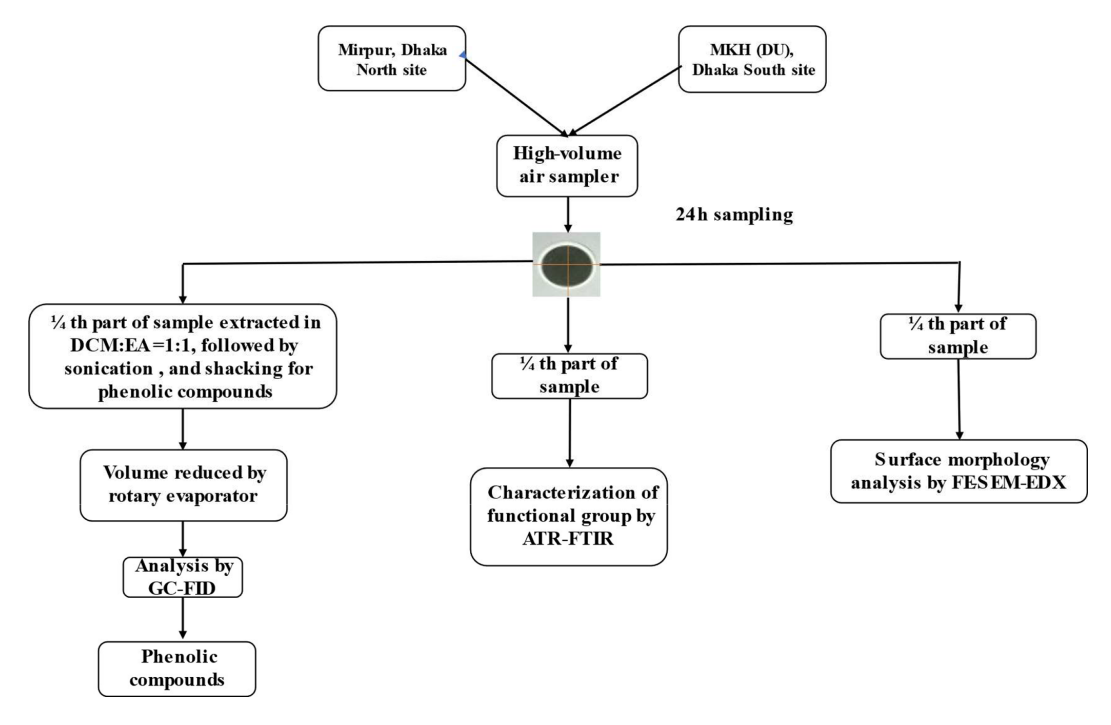


Figure 1. Schematic diagram of the overall sampling and analysis procedure from July 2023 to January 2024 at the Dhaka North site and the Dhaka South site.

2.2 Sample Collection

PM_{2.5} samples were collected using a High-Volume Air Sampler equipped with a PM_{2.5} impactor, operating at a flow rate of 16.7 L min⁻¹, and PM_{2.5} particulates were captured on Quartz filter paper (Gelman, Membrane Filters, type TISSU Quartz 2500QAT-UP, 47 mm diameter). Before sampling, each Quartz filter was heated at 800 °C for 4 h in a furnace to remove any organic impurities. Sampling was conducted simultaneously at both locations (Dhaka South and Dhaka North sites) from July 2023 to January 2024. Each month, four samples were collected from both sites. The sampling period was 24 h. In total, 26 samples, including blanks, were collected from each site. The PM_{2.5} mass was determined by calculating the difference between the weight of the blank filter and the PM_{2.5}-loaded filter. The total volume of air passing through the filter was calculated using the difference between the initial and final readings of the gas meter. After sampling, each sample was wrapped in aluminum foil, stored in a desiccator to regulate humidity, and finally preserved in a refrigerator at 4 °C until further analysis. Flow diagrams are given below Fig. 1.

Figure 1 illustrates the sampling and analysis workflow. In short, PM_{2.5} samples were collected for 24 h from two locations in Dhaka city. Each PM_{2.5}-loaded filter was divided into four equal parts. One-quarter was extracted and analyzed for phenolic precursors of brown carbon using gas chromatography–flame ionization detection (GC-FID). Another quarter was used to identify functional groups via at-

tenuated total reflectance—Fourier transform infrared spectroscopy (ATR-FTIR). A further quarter was examined for surface morphology and elemental composition using field emission scanning electron microscopy coupled with energy-dispersive X-ray spectroscopy (FESEM-EDX).

2.3 SEM-EDX Analysis

Morphological and chemical analyses of PM2.5 were performed by field emission scanning electron microscopy (FE-SEM, Zeiss Sigma 300 VP with 2 Bruker Quantax Xflash 60 mm² SDD EDS Detectors). To obtain a high-resolution SEM image, each sample was kept in a desiccator for 1 h and then freeze-dried for 6 h to completely remove the moisture. Next, a small section of the filter was precisely severed and arranged on a sample holder using carbon nanotape. The sample surface was subjected to gold sputtering to enhance its conductivity. Due to the presence of non-conducting particles on the surface, the electron beam will collide with the sample, resulting in the accumulation of charge and causing a charging effect that leads to fuzzy pictures, which were minimized by gold sputtering. The microscope is controlled entirely by the SmartSEM software suite developed by Zeiss. After gold sputtering under reduced pressure, the sample holder was inserted into the chamber of the SEM-EDX instrument. Air from the chamber was evacuated. When the pressure was reduced below $\sim 0.009 \, \text{Pa}$, extra high tension (EHT) was enabled. SEM image was obtained with an EHT value of 2.0 kV, and EDX was performed with an EHT value

ranging from 10–15 kV. The SDD detector was utilized for EDX analysis. For obtaining the EDX report ESPRIT Spectrum software package was used. The images obtained from SEM and EDX were analyzed by the ImageJ software package. For the morphology study, samples collected on filters may introduce positive artifacts and uncertainties due to the fiber structure of the filters. However, SEM-EDX analysis of these filter samples has been widely employed for the morphological and elemental characterization of individual airborne particles (Park et al., 2023).

2.4 ATR-FTIR analysis

An attenuated total reflection-Fourier transform infrared (ATR-FTIR) spectrometer (Shimadzu, IRPrestige-21, Japan) was utilized to examine the chemical functional group of brown carbon according to Hossen et al. (2023). IR spectra of the samples were obtained within the range of wave number 700–4000 cm⁻¹. Since an ATR probe was utilized in ATR-FTIR, sample preparation was not needed. It is a non-destructive process. During ATR-FTIR analysis, the sample was kept on the crystal (ATR probe), which is composed of high refractive index materials such as AgCl and Si. In this process, infrared (IR) radiation incident on the crystal interacts with the sample on its surface.

2.5 Sample Extraction and Chemical Analysis

To identify and quantify of phenolic precursors of BrC, half of each sample filter paper was cut into small pieces and taken into a conical flask. Then added 30.0 mL of solvent 1:1 (dichloromethane: ethylacetate) and kept it to soak overnight for better extraction. After 24 h, each sample was sonicated for 40 min at 30 °C, followed by shaking for 40 min in an orbital shaker. During the extraction process mouth of the conical flask is completely closed by a cap. The extracted solution was filtered by a syringe filter (PTFE, 0.45 µm). The volume was reduced to approximately 1.0 mL by the rotary evaporator. The final extracted samples were kept in the refrigerator at 4 °C until analysis in a gas chromatographyflame ionization detector (GC-FID). The phenolic precursors of BrC in the extracted sample solutions were identified and quantified by gas chromatography coupled with flame ionization detector (GC-FID) (model: Varian 450-GC, column: VF-5 ms (30 m \times 0.25 mm, ID 0.25 μ m), carrier gas: N₂, Air, H₂, detector temperature: 280 °C, Split ratio: 20, injection volume: 1.0 μL, column flow: 1.2 mL min⁻¹, column temperature: Initial 60 °C (2 min hold), 180 °C (8 °C ram min⁻¹), 180 °C (10 °C ram min⁻¹) 4 min hold, total run time: 27 min).

Standard solution of seven phenolic compounds, such as Phenol (MERCK-Schuchardt), 2-methylphenol (MERCK-Schuchardt), 3-methylphenol (MERCK-Schuchardt), 2-methoxyphenol (MERCK-Schuchardt), 2,4-dimethylphenol (MERCK-Schuchardt), 2-hydroxyphenol (MERCK-Schuchardt) was

prepared using the solvent 1:1 dichloromethane and ethylacetate. Also prepared a mixed standard including these seven standard phenolic compounds. The concentrations of the prepared standard solution were 0.5, 2.5, 5.0, 10.0, 20.0, 40.0, 60.0, 80.0, and 100.0 ppm. At first run the individual standard solution to identify the retention time of target compounds. Then the mixed standard solution was injected into the gas chromatography to separate the individual phenolic compounds. The presence of phenolic compounds in the ambient sample was identified by the presence of a peak at a characteristic retention time in the sample chromatogram compared to that of the chromatogram of the standard solution. On the other hand, the quantitative analysis was conducted by comparing the peak areas of the compounds to those of a standard solution, achieved through the creation of a calibration curve (Fig. S2). Method validation, including the limit of detection (LOD), limit of quantification (LOQ), and recovery rate, was also carried out for this method of quantification of phenolic precursor. The details are described in the Supplement in Sects. S2–S3. In a brief, the recovery experiment was carried out in three samples by spiking a known amount of standard solution. A blank sample and the two samples that gave very little signal/peak in the chromatogram were used as a sample matrix for the recovery test. A known amount of standard solutions was spiked to the filter sample and allowed the sample to stand for an hour to let the phenolic compound be absorbed into the filter matrix. Then extract this spiked sample by the same process of sample extraction. The average recovery rate of the samples was 85 % which is in the acceptable range (Table S1 in the Supplement).

2.6 Nitration Experiment of Catechol to Formation of Light-Absorbing Product

Nitrophenols are the major component of light-absorbing atmospheric organic aerosol, commonly referred as BrC. The primary constituent of BrC is the nitroaromatic compounds, which account for around 40 %-60 % of the total BrC composition. Most of the nitrophenol formation pathways involve the reactions of phenolic compounds with NO₃ and NO₂ in the gas phase in the ambient atmosphere (Wang et al., 2023). Aqueous phase nitration of 1,2-dihydroxy phenol (catechol) forms a major component of brown carbon, such as 4nitrocatechol. Catechol is produced from biomass burning and vehicle emissions. This catechol reacts with nitrous acid in the aqueous phase to form secondary aerosol nitrophenol, which is the major light-absorbing component of organic aerosol. Multiple investigations have demonstrated the significant involvement of NOx in the creation of nitroaromatic compounds (Chow et al., 2016). However, this study presents a method for the production of nitro-aromatic compounds by simple aqueous phase nitration of 2-hydroxyphenol (catechol).

Table 1. List of required reagents for the laboratory experiments to study the formation of nitro-aromatic compounds.

S/N	Reagents	Required Concentration
1.	Catechol (1,2-dihydroxybenzene), $C_6H_4(OH)_2$	1 mM
2.	Sodium Nitrite, NaNO ₂	1 mM
3.	Sulfuric Acid, H ₂ SO ₄	0.1 M
4.	Ammonia Buffer (pH \sim 8) & 6 % $\rm H_2O_2$	Used for alkaline conditions
5.	Hydrogen Peroxide, H ₂ O ₂	6 %

For the nitration reaction, a solution of 1 mM 1,2-dihydroxybenzene and 1 mM NaNO2 is prepared by deionized water in a 50 mL volumetric flask. The 1 : 1 ratio of catechol and sodium nitrite undergoes a chemical reaction both in acidic (pH = 3–4, pH adjusted by 0.1 M $\rm H_2SO_4$ and NaOH) and alkaline medium (used ammonia buffer to maintain pH \sim 9, and $\rm H_2O_2$, which facilitates more $\rm NO_2^+$) to form nitrated phenol. The pH of the solution was measured by a pH meter (model L-510, voltage DC 5V, S/N PK51028202310104). During the reaction continuously measured the absorbance at different times and observed the change of absorbance with time.

Reaction:

3 Results and Discussion

3.1 Morphological Study of PM_{2.5}

In this research investigated the surface elements that are most prevalent in the Earth's atmosphere. The chemical components of $PM_{2.5}$ were categorized into distinct categories according to their morphology, as indicated by the SEM images (Fig. 2a–c). It shows that $PM_{2.5}$ particles exhibit predominantly irregular, aggregate, and chain-like morphologies. Most individual particles are $\leq 2.5\,\mu m$, while aggregates and chain-like structures range from 1.88 to 4.99 μm (Fig. 2c). Such coarse aggregates indicate particle growth through coagulation/agglomeration of smaller particles and the condensation of vapours onto pre-existing seed particles, rather than formation by fresh homogeneous nucleation (Lee et al., 2019). Lots of pre-existing particles in the atmosphere

Table 2. Relative abundance of surface elements in PM_{2.5} obtained from Energy Dispersive X-ray Spectroscopy.

Elements	Atomic No.	Weight %	
С	12	29.84	
O	16	44.61	
Al	13	0.62	
Na	11	2.96	
K	19	0.63	
N	7	0.02	
S	16	0.61	
Ca	20	0.55	
Cr	24	0.01	
Pb	82	0.04	
As	33	0.06	
Hg	80	0.09	

are released from the combustion event of biomass in our daily life, fossil fuels, emissions from vehicles, and other sources. As a result, the gaseous pollutants in the atmosphere (NO_x, SO_x, NH_3, etc) undergo heterogeneous condensation on the surface of the pre-existing particle to form aggregates, chain-like aerosols of sulfate and nitrate. The morphology of the particles in PM_{2.5}, including diameter and shape, is similar in Dhaka North and Dhaka South sites, but the surface chemical compositions are varied with season and sampling locations. The observed surface morphologies of aerosol particles, including irregular, aggregate, and chain-like structures, play a significant role in the formation and optical properties of BrC. These morphologies provide a large reactive surface area that facilitates the heterogeneous adsorption and condensation of gaseous phenolic precursors and other organic compounds onto existing particles. Such interactions promote the chemical aging processes like nitration and oxidation, which enhance the light-absorbing capacity characteristic of BrC (Hossen et al., 2025).

3.2 Surface Elements Analysis

According to the EDX data, surface chemical compositions were categorized into carbonaceous, mineral dust, and trace metal. Table 2 shows that the quantity of carbon (C) and oxygen (O) was very high in PM_{2.5}, along with varying amounts of minerals (Ca, Fe, K, Al), sulfur, nitrogen, and trace metals (As, Cr, Cd, Pb, Hg). The sequence of carbonaceous elements (C, O, N, and S) in Dhaka North & South sites was O > C > N > S.

Their possible emission sources are the combustion of fossil fuels and biomass burning. Sulfur dioxide (containing S) is primarily emitted from coal combustion, while nitrogen dioxide (containing N) mainly originates from agricultural land and fertilizers. The sequence of abundance for minerals is Al > Ca > K > Fe. These minerals originate from mineral dust, biomass burning, and industrial waste. The trace

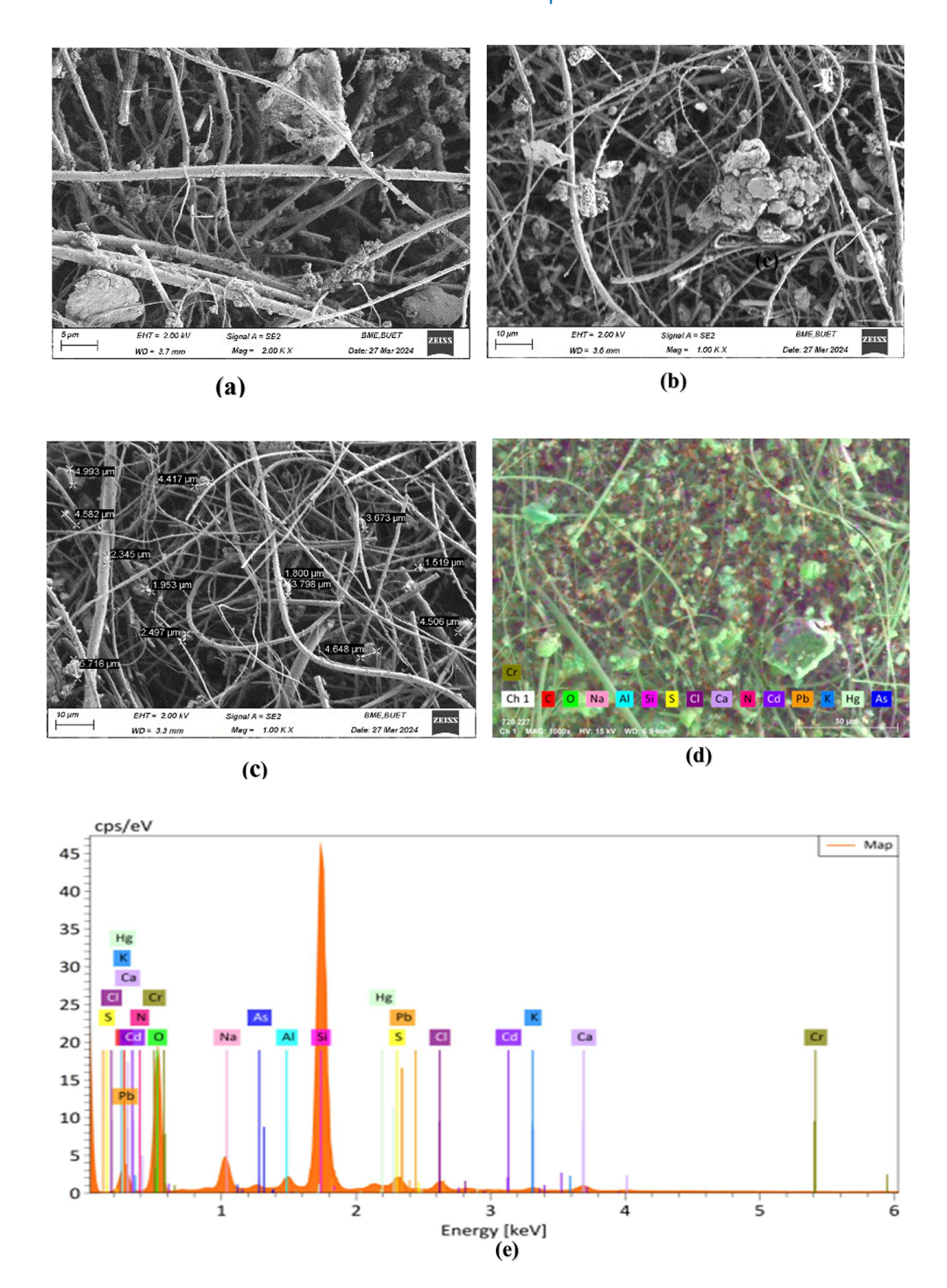


Figure 2. Scanning Electron Microscope (SEM) images of $PM_{2.5}$ loaded filter in (a) Dhaka North site, (b) Dhaka, South site, and (c) size distribution of particles in $PM_{2.5}$ loaded sample; (d) Energy Dispersive X-ray Spectroscopy (EDX) mapping, (e) EDX Spectra of $PM_{2.5}$.

heavy metals were present in meager amounts. Among the five harmful trace metals (Hg, Cr, Pb, Cd, As), lead has the highest abundance of surface elements, while the abundance of Hg was the lowest. The composition suggests that particle growth was mainly due to condensation and coagulation,

with mixing of combustion-related and mineral dust aerosols at the sampling sites.

3.3 Characterization of Functional Group

The IR spectra (Fig. S3) demonstrate that the majority of the material comprises the aromatic ring system because

Table 3. Primary band assignments for ATR-FTIR spectra of $PM_{2.5}$ particulate matter.

Range of Wavenumber	Vibrational Assignment
$2500-2000\mathrm{cm}^{-1}$	$C \equiv N$ and $C \equiv C$ bond stretching
$1800-1650\mathrm{cm}^{-1}$	Carbonyl ($C = O$) bond stretching
$1600-1475\mathrm{cm}^{-1}$	Aromatic ring stretching
$1640-1550\mathrm{cm}^{-1}$	Bending of aromatic N-H bond
$1445\mathrm{cm}^{-1}$	Bending of $-CH_3$, $-CH_2$ and
	stretching of aromatic ring
$1355-1315 \mathrm{cm}^{-1}$	R − ONO ₂ organic nitrate stretching
$1440 - 1220 \mathrm{cm}^{-1}$	Bending of C-O-H
$1200-1000\mathrm{cm}^{-1}$	Stretching vibration of $C - O$
$900-690\mathrm{cm}^{-1}$	Out plane bending of aromatic ring

sharp peaks are found at $\sim 1630-1660\,\mathrm{cm}^{-1}$, and $\sim 1440-$ 1460 cm⁻¹. At this range, conjugated double bonds display the IR absorption. Peak obtained at 1600–1690 cm⁻¹, which is most probably the characteristic peak of stretching of the C-O-C bond. The peak at 1500–1600 cm⁻¹ suggested that the stretching of the aromatic ring, which is a common peak in all the PM_{2.5} samples (Table 3). So, it's giving an obvious understanding that the particulate matter contains the aromatic ring with a conjugated double bond. Few samples exhibit a peak at 2400–2500 cm⁻¹ in this range −C≡N and C≡C undergo stretching vibration. The peak at the wave number 1400-1450 cm⁻¹ is the bending of methyl groups and the methylene group. Examining the fingerprint region reveals intriguing characteristics. This investigation identified a substantial number of peaks in the fingerprint region, specifically at 1325 and 1340 cm⁻¹, which indicate the existence of organic nitrate aerosol in PM_{2.5}.

3.4 Identification and Quantification of Phenolic Compounds (precursor of BrC)

3.4.1 Chromatogram of GC-FID Analysis

The chromatogram generated by GC-FID displayed the retention time, peak area, and identified compound. The identity of the unknown compound is ascertained through a comparison of its chromatogram with that of the standard sample. A calibration curve represents quantitative information regarding the identified compound. The chromatogram was given in the Supplement in Sect. S5 (Figs. S4 to S8).

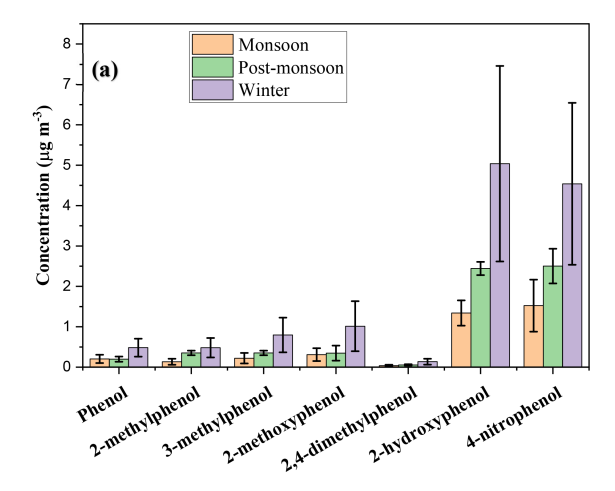
3.4.2 Phenolic Precursor of BrC

The phenolic components serving as primary precursors of BrC include phenol, 4-nitrophenol, methoxy phenol, and cresols (m-cresol, p-cresol, and o-cresol). The precursors are initially emitted from the source as primary aerosols. Figure 3 illustrates that the mean concentration of nitrophenol and catechol in PM_{2.5} was comparatively greater than that

of other phenolic compounds. The average concentrations of nitrophenol in Dhaka South (DU) during the monsoon, postmonsoon, and winter seasons were 1.52 ± 0.64 , 2.50 ± 0.43 , and $4.54 \pm 2.94 \,\mu \text{g m}^{-3}$, respectively. In contrast, at Mirpur, Dhaka North, the concentrations were 1.34 ± 0.09 , 1.65 ± 0.44 , and $1.62 \pm 0.52 \,\mu \text{g m}^{-3}$ during the same seasons. These concentrations were approximately 40 %-70 % lower than the levels observed at the Dhaka South site. In Dhaka South, the second-highest concentration was found to be 2-hydroxyphenol (catechol) with values of 1.34 ± 0.31 , 2.44 ± 0.16 , and $5.04 \pm 3.41 \,\mu g \, m^{-3}$ during the monsoon, post-monsoon, and winter seasons, respectively, while the values recorded at Mirpur were 1.43 ± 0.07 , 1.78 ± 0.53 , and $1.82 \pm 0.51 \,\mu \mathrm{g} \,\mathrm{m}^{-3}$, respectively (Table S9). The levels of phenol and methyl derivatives of phenol were significantly lower compared to nitrophenol. In Mirpur, Dhaka North, the concentration of 2-hydroxyphenol is higher compared to nitrophenol. This is due to emissions from cooking, burning coal in restaurants, and biomass burning, which directly release 2-hydroxyphenol or catechol. During the winter, the increased combustion of coal and biomass for heating purposes is responsible for the significant rises in phenolic compound concentrations (Wang et al., 2018a). After the release of 2hydroxyphenol, it undergoes a secondary chemical reaction with NOx or aqueous nitrous acid in the atmosphere to form nitrophenol.

The average concentration of phenol in Dhaka city was $0.15\pm0.08,\ 0.17\pm0.04,\$ and $0.30\pm0.25\$ µg m $^{-3}$ in monsoon, post-monsoon, and winter seasons, respectively. The concentration of phenol in the winter season was comparatively higher than in other seasons because the major emission source of phenol is biomass burning. And most of the biomass burning occurred in the winter seasons. Among the methyl derivatives measured in Dhaka, Bangladesh, from July 2023 to January 2024, 2-methoxyphenol exhibited the highest concentration at $0.42\pm0.29\$ µg m $^{-3}$, while 2,4-dimethylphenol had the lowest concentration, recorded at $0.05\pm0.04\$ µg m $^{-3}$. The high concentration of 2-methoxyphenol, which is directly emitted from biomass burning, likely indicates frequent biomass burning activities occurring near the sampling site in Dhaka, Bangladesh.

In contrast to findings from other research, the mean concentration of nitrated phenols observed in this study is significantly greater than the concentration of phenol. Li et al. (2020) reported that the average concentration of phenol in urban Jinan, China was $(1.67\pm0.37)\times10^{-2}$, $(7.1\pm2.6)\times10^{-3}$, and $(2.6\pm0.4)\times10^{-3}$ µg m⁻³ in winter, spring, and summer, respectively. Delhomme et al. (2010) quantified the phenolic and nitrated compounds in the ambient air and obtained the concentrations of phenol, m-cresol (3-methylphenol), and o-cresol (2-methylphenol) were 1.04×10^{-2} , 2.20×10^{-3} , 1.20×10^{-3} µg m⁻³, respectively, in an urban site. Figure 3 also shows that season and sampling location had an impact on the fractional compositions of phenolic compounds. The most prevalent phenolic compounds



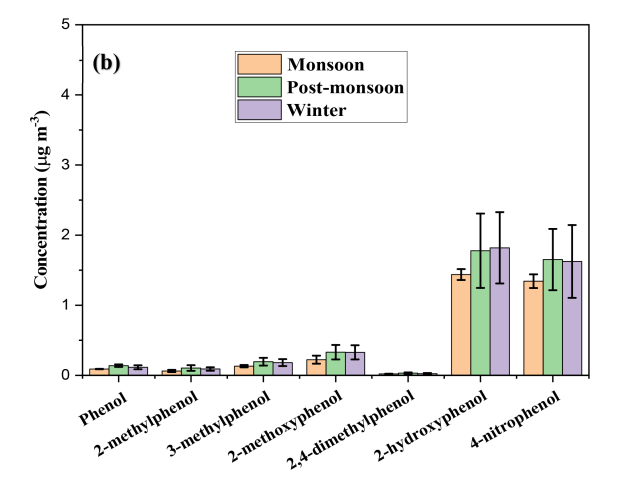


Figure 3. Variation of concentration of phenolic compounds in **(a)** Dhaka, South and **(b)** Dhaka North site during monsoon, postmonsoon and winter.

in PM_{2.5} during the monsoon, post-monsoon, and winter seasons were 4-nitrophenol and 2-hydroxyphenol, which accounted for 37 %–40 % and 39 %–41 % of the quantified phenolic precursors, respectively, in Dhaka city from July 2023 to January 2024. 2,4-dimethylphenol lies in the lowest portion among the identified phenolic compounds, accounting for 0.8 %–1 % of the total identified phenolic precursors. The contribution of 3-methylphenol increased by 0.2 % from the monsoon to the post-monsoon season and saw a further increase of 0.5 % during winter (Fig. 3).

Previous research found that catechols and 4-nitrophenol were the most abundant phenolic compounds detected in Jinan and Beijing, with the highest observed concentrations (Wang et al., 2018b; Wang et al., 2019). The prevalence of 4-nitrophenol and 2-hydroxyphenol in both Dhaka South and Dhaka North may be attributed to primary emissions, such as combustion activities, as well as the subsequent formation of precursors of BrC. The high value of nitrophenol also indicated the higher concentration of NO_x in the atmosphere.

Liu et al. (2016) reported an enhancement in the light absorption of secondary organic aerosols (SOA) when exposed to elevated NO_x levels and moderate humidity, attributing this primarily to the presence of nitro-aromatic compounds as key chromophores. According to Laskin et al. (2025), the optical characteristics of BrC can be altered through atmospheric aging, including processes such as photolysis and multiphase reactions that either produce or degrade light-absorbing species.

3.4.3 Correlation analysis of phenolic compounds

The correlation analysis (Table 4) shows that most of the compounds exhibit strong correlations with each other (close to 1), indicating that they behave similarly, possibly due to shared structural or chemical properties. This analysis also indicated that most of the phenolic compounds emitted from the same sources were most probably it was biomass burning and vehicle emissions. r = 0.974 for 4-NPh and 2-HPh, and r = 0.9879 for Ph and 2 MPh, suggesting that an extremely strong positive correlation exists between each pair, and they behave very similarly. There is a moderate to significant association between 2,4-dimethylphenol (2,4-DMPh) and 2methoxyphenol (2-MOPh) (r = 0.7708). Their relationship is not as strongly connected as some other pairs in Table 4. 4-NPh and 2,4-DMPh show a moderate positive correlation. They may exhibit different behaviors. 2,4-DMPh shows less correlation with other phenolic compounds.

3.5 Formation of light-absorbing nitro-aromatic compounds

In our study, we quantified several common BrC precursors in the ambient atmosphere. Among them, 2-hydroxyphenol and 4-nitrophenol were found in the highest concentrations in our sampling area, both of which are well-known products of biomass burning. To gain a better understanding of the possible formation processes of nitroaromatic compounds under atmospheric conditions, we conducted controlled aqueousphase nitration experiments in the laboratory.

In these experiments, catechol (2-hydroxyphenol), selected because it was the most abundant precursor detected in our samples, was reacted with sodium nitrite under both acidic conditions (pH adjusted using H_2SO_4 and NaOH) and basic conditions (pH adjusted using ammonia buffer, with H_2O_2 added to enhance NO_2^- production) to form light absorbing nitro aromatic compound.

3.5.1 UV-visible light absorption properties of the catechol-nitrite reaction system

The catechol (2-hydroxyphenol) absorbs the UV-visible light at 280 nm (peak at 280 nm) (Scalzone et al., 2020). When it reacted with the sodium nitrite in the presence of H_2SO_4 , the peak (λ_{max}) was shifted to a longer wavelength. This shift

Table 4. Correlation analysis of phenolic compounds.

	4-NPh	2-HPh	Ph	2-MPh	3-MPh	2-MOPh	2,4-DMPh
4-NPh	1						
2-HPh	0.974	1					
Ph	0.900	0.889	1				
2-MPh	0.907	0.9199	0.9879	1			
3-MPh	0.957	0.9558	0.9813	0.9898	1		
2-MOPh	0.915	0.9442	0.966	0.9701	0.9723	1	
2,4-DMPh	0.662	0.6809	0.8341	0.8659	0.8077	0.7708	1

Note: 4-NPh = 4-nitrophenol, 2-HPh = 2-hydroxyphenol, Ph = phenol, 2-MPh = 2-methylphenol, 3-MPh = 3-methylphenol, 2-MOPh = 2-methoxyphenol, 2, 4-DMPh = 2, 4-dimethylphenol.

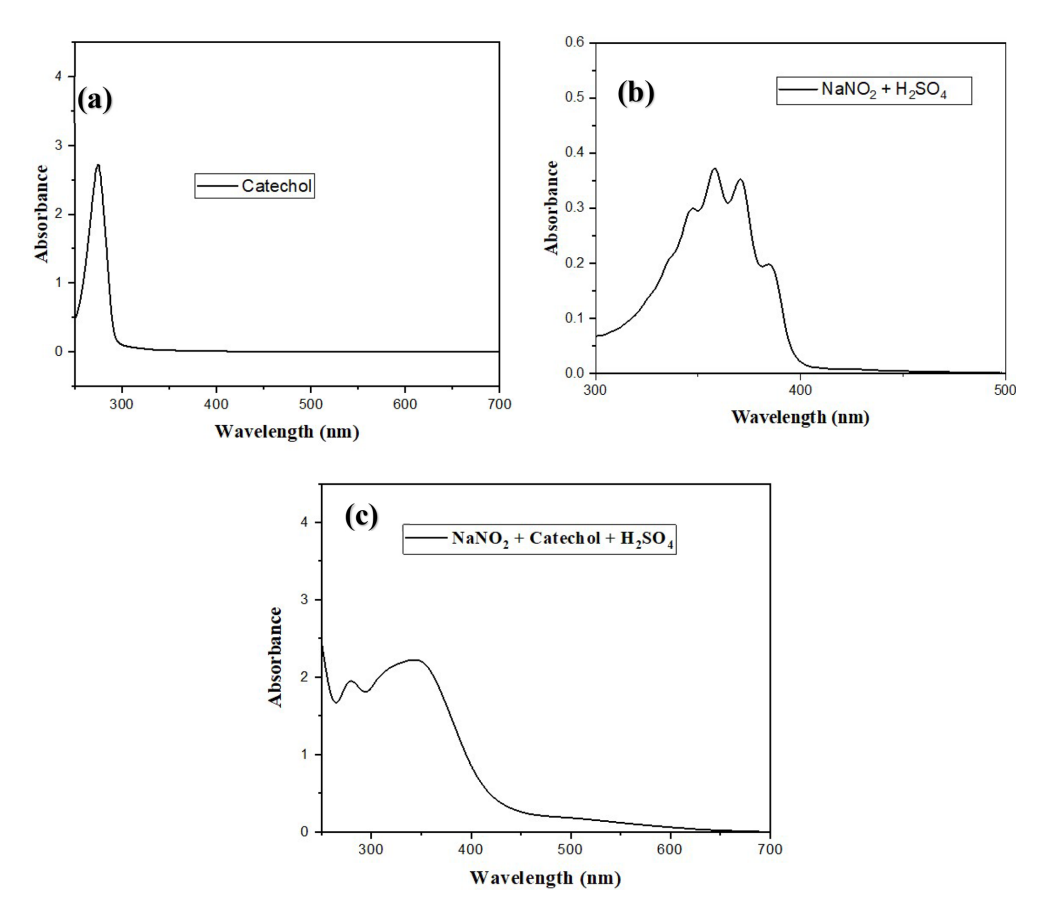


Figure 4. Absorbance of (a) single catechol, $\lambda_{max} = 275$ nm, (b) NaNO₂+ H₂SO₄, and (c) reaction system (catechol-nitrite).

of λ_{max} indicated that there was an interaction between 2-hydroxyphenol and the nitrite ions in the reaction system (Fig. 4).

PM At pH = 3.5, the absorbance gradually increases with time in the wavelength range from 300–700 nm, and the λ_{max} shifts to a shorter wavelength with time increase. Initially, at 1 min the λ_{max} obtained at 355 nm then as time increased the absorbance increased gradually and the λ_{max} shifted to a shorter wavelength such as 338 nm after half an hour and no change further increase in time (Fig. 5a). It is clear from this change that the nitro group has been added to the aromatic

ring, leading to an increase in absorption and a shift in the position of the peak.

At the early stage (1 min), as shown in Fig. 5a, the spectrum is dominated by the characteristic $\pi \to \pi^*$ transition of the aromatic ring, centered near 270–280 nm, with relatively low intensity in the higher wavelength region. As the reaction proceeds, both the main aromatic band and a second band in the 300–350 nm region gradually increase in intensity, with the latter showing a slight bathochromic shift. This hyperchromic effect and modest red shift are consistent with the formation of nitro-substituted aromatic compounds such as

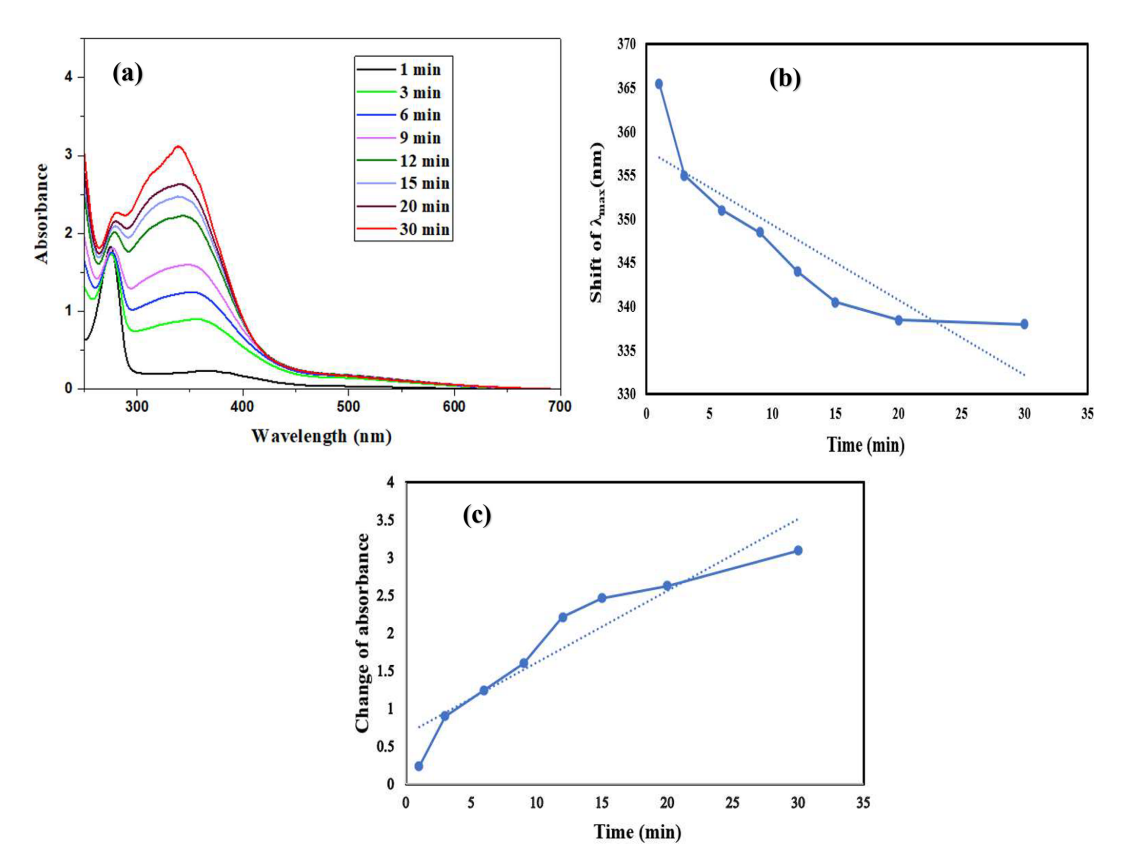


Figure 5. (a) Change of the absorbance with times of the reaction system containing 1 mM 2-hydroxyphenol and 1 mM NaNO₂ at pH = 3.5. A distinct color denotes the duration of the sample run in the ultraviolet-visible spectrophotometer. The initial reactant contribution was subtracted from each spectrum. (b) Shift of λ_{max} with time, and (c) Change of absorbance with time.

o- or p-nitrophenol. The strong electron-withdrawing nature of the nitro group extends conjugation and enhances $n \to \pi^*$ and charge-transfer transitions, leading to stronger and slightly longer wavelength absorption than the parent phenol. The continuous increase in absorbance with time, without any later decline, confirms the accumulation of these nitroaromatic products in solution. This spectral change therefore provides strong evidence that the reaction proceeds through electrophilic aromatic substitution of 2-hydroxyphenol by nitronium ions generated from NaNO2 in the acidic medium, yielding stable nitrophenol derivatives with enhanced UV absorption.

3.5.2 Reaction in alkaline medium

At high pH, nitrite remains primarily in the form of NO_2^- , and the formation of electrophiles such as HONO, NO_2^+ , or N_2O_3 is strongly suppressed. Although phenolates are highly activating toward substitution, the lack of these electrophilic species makes aromatic nitration largely ineffective. However, the presence of peroxide facilitates the formation of NO_2^+ .

Figure 6, the UV–Vis spectra of the $NaNO_2$ –2-hydroxyphenol system in alkaline medium with H_2O_2 show

a time-dependent evolution of absorption features, indicating the formation of light-absorbing products. Initially, the spectrum is dominated by the characteristic UV absorption of phenolate anions (\sim 280–300 nm), but with reaction time (0–15 min), the peak intensity increases and a broad shoulder emerges and intensifies in the 400-450 nm region. This indicated the completed protonated form of nitrophenol (Syedd-León et al., 2020). This bathochromic shift and visible-range growth reflect the formation of conjugated nitroaromatic and quinone-like species with extended π -systems, likely via oxidation of phenolate by HO₂/oxidants and subsequent nitration by reactive nitrogen species from nitrite. The progressive increase in visible absorption is consistent with the generation of chromophoric, BrC-type products with potential atmospheric light-absorbing properties. These spectral changes strongly suggest nitro-substituted aromatic and quinone-type chromophores are forming in the system.

Under acidic conditions, nitrite generates the potent electrophile NO_2^+ (via HNO_2/HNO_2^+) and N_2O_3/NO^+ equilibria. The activated aromatic ring of phenol or catechol then undergoes rate-determining electrophilic attack by NO_2^+ to form the Wheland (σ) intermediate, directed ortho/para by the OH group(s). Subsequent deprotonation restores aromaticity, yielding the nitroaromatic product. The reaction mech-

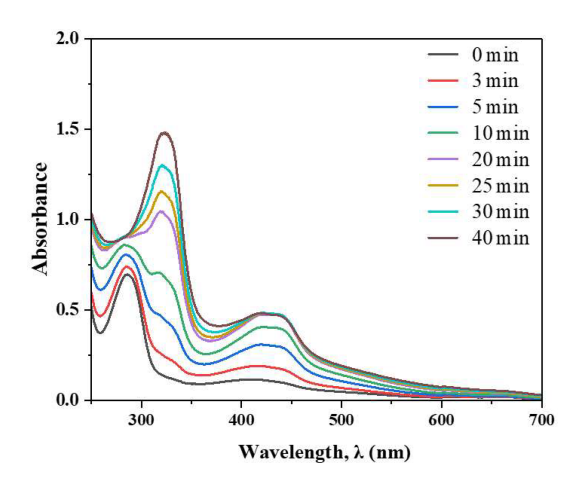


Figure 6. UV-visible absorption spectra of the nitrite-catechol reaction system in alkaline medium, pH \sim 7–8 to form a light-absorbing nitro aromatic compound.

anism of the nitration of aromatic compounds takes place through the reaction with an aqueous nitrite solution. Esteves et al. (2003) have also suggested that the exceedingly potent electrophile NO_2^+ facilitated the reaction at a low pH. The NO_2^+ electrophile attacks the benzene ring and forms a C-N bond. According to Wang et al. (2023) HONO acts as an electrophile in the aqueous nitration of catechol (2-hydroxybenzene). This explains the accelerated nitration rate in acidic environments, as HONO, being a stronger electrophile than NO_2^- , is more readily formed at lower pH levels.

Under alkaline conditions, nitration is generally unfavorable. At high pH, nitrite remains primarily in the form of NO_2^- , and the formation of electrophiles such as HONO, NO_2^+ , or N_2O_3 is strongly suppressed. Although phenolates are highly activating toward substitution, the lack of these electrophilic species makes aromatic nitration largely ineffective. However, the presence of peroxide facilitates the formation of NO_2^+ .

In the atmosphere, a similar pathway occurs inside aqueous aerosol droplets or cloud/fog water, where phenolic compounds (e.g., catechol) are taken up. These droplets adsorb NO₂ and interact with OH radicals under sunlight, generating reactive nitrogen species (HONO, NO₂⁺, peroxynitrite) that nitrate and oxidize the phenolic precursors. This process yields nitro-aromatic and quinone-type chromophores, which extend absorption into the visible range (Yang et al., 2023). Thus, the laboratory results directly mimic the aqueous-phase reactions in atmospheric droplets that lead to the formation of light-absorbing BrC.

4 Conclusions

This study provides comprehensive insights into the compositions, surface elements, and formation mechanism of

brown carbon in the atmosphere of Dhaka, Bangladesh, through the identification and quantification of seven key phenolic precursors and an aqueous-phase nitration experiment. We observed that PM_{2.5} predominantly exhibited spherical, irregular, and chain-like morphologies, with carbonaceous (C, O, N, S), mineral (Ca, Fe, K, Al), and trace elements (Pb, Cr, Hg, Cd, As) identified on their surfaces. Attenuated Total Reflectance - Fourier Transform Infrared Spectroscopy (ATR-FTIR) analysis revealed prominent functional groups, including carbonyls, nitro groups (-NO₂), and aromatic conjugated systems, suggesting the presence of complex organic structures. Among the phenolic precursors, 4-nitrophenol $(2.20 \pm 1.21 \,\mu\mathrm{g m}^{-3})$ and 2-hydroxyphenol $(2.31 \pm 1.39 \,\mathrm{\mu g \, m^{-3}})$ showed the highest concentrations, especially during winter. A strong seasonal and spatial variation was evident, with higher levels in Dhaka South, indicating the influence of urban emissions and combustion activities. Correlation analysis revealed strong positive relationships among most compounds (r > 0.9), suggesting shared emission sources such as biomass and fossil fuel combustion. These findings suggest that phenolic compounds are not only abundant in the urban air of Dhaka but also highly reactive, forming nitrated derivatives such as 4-nitrophenol that contribute substantially to brown carbon. The detection of nitrated and hydroxylated phenols further highlights their transformation via atmospheric oxidation processes. The similarity in chemical behavior and high co-occurrence among these phenolic compounds confirms their common origin and potential for secondary aerosol formation.

Compared to other urban regions like Jinan, China, and Strasbourg, France, the concentrations of phenolic and nitrated phenolic compounds in Dhaka are substantially higher, likely due to more intense and unregulated combustion activities (Li et al., 2020; Delhomme et al., 2010). Our findings align with prior studies (e.g., Wang et al., 2018b; Li et al., 2022) identifying catechols and nitrophenols as dominant brown carbon components but extend the understanding by quantifying these compounds across seasons and locations within a South Asian megacity.

While this study presents robust data on PM_{2.5} composition and brown carbon precursors, limitations include the relatively short sampling period and limited spatial coverage. Additionally, although aqueous-phase nitration experiments were conducted, the ambient contribution of such processes remains to be quantified. Future studies should explore broader geographic regions, perform year-round monitoring, and couple laboratory findings with atmospheric modeling for deeper mechanistic insights. The results underscore the significant contribution of phenolic and nitrated phenolic compounds to atmospheric brown carbon in Dhaka, with implications for both regional air quality and climate forcing. The demonstrated aqueous-phase nitration pathway of catechol at acidic pH suggests a potentially underappreciated route for brown carbon formation under humid and pol-

luted conditions. This highlights the importance of regulating combustion-related emissions and considering aqueousphase chemistry in climate models to accurately assess the radiative effects of organic aerosols.

Data availability. Data will be available upon request.

Supplement. The supplement related to this article is available online at https://doi.org/10.5194/acp-25-14629-2025-supplement.

Author contributions. MAH: Conceptualization, Sampling, Methodology, Chemical analysis, Writing-original draft, Review & editing; MHS: Chemical Analysis; ARMT: Chemical Analysis, Methodology, and Supervision; MFE: Chemical Analysis; AS: Conceptualization, Review & editing, Supervision.

Competing interests. The contact author has declared that none of the authors has any competing interests.

Disclaimer. Publisher's note: Copernicus Publications remains neutral with regard to jurisdictional claims made in the text, published maps, institutional affiliations, or any other geographical representation in this paper. While Copernicus Publications makes every effort to include appropriate place names, the final responsibility lies with the authors. Views expressed in the text are those of the authors and do not necessarily reflect the views of the publisher.

Acknowledgements. The authors express their gratitude to the Department of Chemistry, University of Dhaka, and the Environmental and Organic Chemistry Laboratory, Chemistry Division, Atomic Energy Centre Dhaka, Bangladesh.

Financial support. This research has been supported by the Department of Chemistry, University of Dhaka, Bangladesh.

Review statement. This paper was edited by Sergey A. Nizkorodov and reviewed by two anonymous referees.

References

- Andreozzi, R., Canterino, M., Caprio, V., Di Somma, I., and Sanchirico, R.: Salicylic acid nitration by means of nitric acid/acetic acid system: Chemical and kinetic characterization, Org. Process. Res. Dev., 10, 1199–1204, https://doi.org/10.1021/op060148o, 2006.
- Ankhy, R. S., Roy, S., Nahar, A., Akbor, A., Al-amin Hossen, M., Jeba, F., Safiqul Islam, M., Moniruzzaman, M., and Salam, A.: Optical Characteristics of Brown Carbon in the Atmospheric Particulate Matter of Dhaka, Bangladesh: Analysis of Sol-

- vent Effects and Chromophore Identification, Heliyon, e36213, https://doi.org/10.1016/j.heliyon.2024.e36213, 2024.
- Chow, K. S., Huang, X. H. H., and Yu, J. Z.: Quantification of nitroaromatic compounds in atmospheric fine particulate matter in Hong Kong over 3 years: Field measurement evidence for secondary formation derived from biomass burning emissions, Environmental Chemistry, 13, 665–673, https://doi.org/10.1071/EN15174, 2016.
- Delhomme, O., Morville, S., and Millet, M.: Seasonal and diurnal variations of atmospheric concentrations of phenols and nitrophenols measured in the Strasbourg area, France, Atmos. Pollut. Res., 1, 16–22, https://doi.org/10.5094/APR.2010.003, 2010.
- Esteves, P. M., Carneiro, J. W. de M., Cardoso, S. P., Barbosa, A. G. H., Laali, K. K., Rasul, G., Prakash, G. K. S., and Olah, G. A.: Unified mechanistic concept of electrophilic aromatic nitration: Convergence of computational results and experimental data, J. Am. Chem. Soc., 125, 4836–4849, https://doi.org/10.1021/ja021307w, 2003.
- Feng, Y., Ramanathan, V., and Kotamarthi, V. R.: Brown carbon: a significant atmospheric absorber of solar radiation?, Atmos. Chem. Phys., 13, 8607–8621, https://doi.org/10.5194/acp-13-8607-2013, 2013.
- Finewax, Z., De Gouw, J. A., and Ziemann, P. J.: Identification and Quantification of 4-Nitrocatechol Formed from OH and NO₃ Radical-Initiated Reactions of Catechol in Air in the Presence of NOx: Implications for Secondary Organic Aerosol Formation from Biomass Burning, Environ. Sci. Technol., 52, 1981–1989, https://doi.org/10.1021/acs.est.7b05864, 2018.
- Harrison, M. A. J., Barra, S., Borghesi, D., Vione, D., Arsene, C., and Iulian Olariu, R.: Nitrated phenols in the atmosphere: A review, Atmos. Environ., 39, 231–248, https://doi.org/10.1016/j.atmosenv.2004.09.044, 2005.
- Heal, M. R., Harrison, M. A. J., and Neil Cape, J.: Aqueous-phase nitration of phenol by N₂O₅ and ClNO₂, Atmos. Environ., 41, 3515–3520, https://doi.org/10.1016/j.atmosenv.2007.02.003, 2007
- Hems, R. F., Schnitzler, E. G., Liu-Kang, C., Cappa, C. D., and Abbatt, J. P. D.: Aging of Atmospheric Brown Carbon Aerosol, ACS Earth and Space Chemistry, 5, 722–748, https://doi.org/10.1021/acsearthspacechem.0c00346, 2021.
- Hossain, M. A., Zaman, S. U., Roy, S., Islam, M. S., Zerin, I., and Salam, A.: Emission of particulate and gaseous air pollutants from municipal solid waste in Dhaka City, Bangladesh, J. Mater. Cycles Waste Manag., 26, 552–561, https://doi.org/10.1007/s10163-023-01855-w, 2024.
- Hossen, M. A. A., Roy, S., Zaman, S. U., and Salam, A.: Emission of water soluble brown carbon from different combustion sources: Optical properties and functional group characterisation, Environ. Res. Commun., 5, https://doi.org/10.1088/2515-7620/acea1d, 2023.
- Hossen, M. A. amin, Roy, S., Nahian, S., Zaman, S. U., Selim, A., and Salam, A.: Spectral characteristics of water-soluble Brown carbon and it's radiative impacts on the atmosphere of Dhaka, Bangladesh, Atmos. Environ., 351, 121185, https://doi.org/10.1016/J.ATMOSENV.2025.121185, 2025.
- Hummel, M., Laus, G., Nerdinger, S., and Schottenberger, H.: Improved synthesis of 3-nitrosalicylic acid, Synth. Commun., 40, 3353–3357, https://doi.org/10.1080/00397910903419852, 2010.

- Iinuma, Y., Böge, O., and Herrmann, H.: Methyl-nitrocatechols: Atmospheric tracer compounds for biomass burning secondary organic aerosols, Environ. Sci. Technol., 44, 8453–8459, https://doi.org/10.1021/es102938a, 2010.
- Kumar, P., Hama, S., Nogueira, T., Abbass, R. A., Brand, V. S., Andrade, M. de F., Asfaw, A., Aziz, K. H., Cao, S. J., El-Gendy, A., Islam, S., Jeba, F., Khare, M., Mamuya, S. H., Martinez, J., Meng, M. R., Morawska, L., Muula, A. S., Shiva Nagendra, S. M., Ngowi, A. V., Omer, K., Olaya, Y., Osano, P., and Salam, A.: In-car particulate matter exposure across ten global cities, Science of the Total Environment, 750, https://doi.org/10.1016/j.scitotenv.2020.141395, 2021.
- Laskin, A., Laskin, J., and Nizkorodov, S. A.: Chemistry of Atmospheric Brown Carbon, Chemical Reviews, 115, 4335–4382, https://doi.org/10.1021/cr5006167, 2015.
- Laskin, A., West, C. P., and Hettiyadura, A. P. S.: Molecular insights into the composition, sources, and aging of atmospheric brown carbon, Chemical Society Reviews, 54, https://doi.org/10.1039/d3cs00609c, 2025.
- Lee, H. J., Aiona, P. K., Laskin, A., Laskin, J., and Nizkorodov, S. A.: Effect of solar radiation on the optical properties and molecular composition of laboratory proxies of atmospheric brown carbon, Environ. Sci. Technol., 48, 10217–10226, https://doi.org/10.1021/es502515r, 2014.
- Lee, S. H., Gordon, H., Yu, H., Lehtipalo, K., Haley, R., Li, Y., and Zhang, R.: New Particle Formation in the Atmosphere: From Molecular Clusters to Global Climate, Journal of Geophysical Research: Atmospheres, 124, 7098–7133, https://doi.org/10.1029/2018JD029356, 2019.
- Li, M., Wang, X., Lu, C., Li, R., Zhang, J., Dong, S., Yang, L., Xue, L., Chen, J., and Wang, W.: Nitrated phenols and the phenolic precursors in the atmosphere in urban Jinan, China, Science of the Total Environment, 714, https://doi.org/10.1016/j.scitotenv.2020.136760, 2020.
- Li, M., Wang, X., Zhao, Y., Du, P., Li, H., Li, J., Shen, H., Liu, Z., Jiang, Y., Chen, J., Bi, Y., Zhao, Y., Xue, L., Wang, Y., Chen, J., and Wang, W.: Atmospheric Nitrated Phenolic Compounds in Particle, Gaseous, and Aqueous Phases During Cloud Events at a Mountain Site in North China: Distribution Characteristics and Aqueous-Phase Formation, Journal of Geophysical Research: Atmospheres, 127, https://doi.org/10.1029/2022JD037130, 2022.
- Liu, D., He, C., Schwarz, J. P., and Wang, X.: Lifecycle of lightabsorbing carbonaceous aerosols in the atmosphere, NPJ Clim. Atmos. Sci., 3, 40, https://doi.org/10.1038/s41612-020-00145-8, 2020.
- Liu, J., Lin, P., Laskin, A., Laskin, J., Kathmann, S. M., Wise, M., Caylor, R., Imholt, F., Selimovic, V., and Shilling, J. E.: Optical properties and aging of light-absorbing secondary organic aerosol, Atmos. Chem. Phys., 16, 12815–12827, https://doi.org/10.5194/acp-16-12815-2016, 2016.
- Nakao, S., Clark, C., Tang, P., Sato, K., and Cocker III, D.: Secondary organic aerosol formation from phenolic compounds in the absence of NO_x, Atmos. Chem. Phys., 11, 10649–10660, https://doi.org/10.5194/acp-11-10649-2011, 2011.
- Park, J. I., Kim, M. S., Yeo, M., Choi, M., Lee, J. Y., Natsagdorj, A., Kim, C., Song, M., and Jang, K. S.: Chemical and morphological characterization by SEM-EDS of PM_{2.5} collected

- during winter in Ulaanbaatar, Mongolia, Atmos. Environ., 303, https://doi.org/10.1016/j.atmosenv.2023.119752, 2023.
- Rahman, M. M., Rahaman, M. S., Islam, M. R., Rahman, F., Mithi, F. M., Alqahtani, T., Almikhlafi, M. A., Alghamdi, S. Q., Alruwaili, A. S., Hossain, M. S., Ahmed, M., Das, R., Emran, T. B., and Uddin, M. S.: Role of phenolic compounds in human disease: Current knowledge and future prospects, Molecules, 27, 233, https://doi.org/10.3390/molecules27010233, 2022.
- Runa, F., Islam, M. S., Jeba, F., and Salam, A.: Light absorption properties of brown carbon from biomass burning emissions, Environmental Science and Pollution Research, 29, 21012–21022, https://doi.org/10.1007/s11356-021-17220-z, 2022.
- Scalzone, A., Bonifacio, M. A., Cometa, S., Cucinotta, F., De Giglio, E., Ferreira, A. M., and Gentile, P.: pH-Triggered Adhesiveness and Cohesiveness of Chondroitin Sulfate-Catechol Biopolymer for Biomedical Applications, Front. Bioeng. Biotechnol., 8, https://doi.org/10.3389/fbioe.2020.00712, 2020.
- Syedd-León, R., Sandoval-Barrantes, M., Trimiño-Vásquez, H., Villegas-Peñaranda, L. R., and Rodríguez-Rodríguez, G.: Revisiting the fundamentals of p-nitrophenol analysis for its application in the quantification of lipases activity, A graphical update, Uniciencia, 34, 31–42, https://doi.org/10.15359/RU.34-2.2, 2020.
- Wang, H., Gao, Y., Wang, S., Wu, X., Liu, Y., Li, X., Huang, D., Lou, S., Wu, Z., Guo, S., Jing, S., Li, Y., Huang, C., Tyndall, G. S., Orlando, J. J., and Zhang, X.: Atmospheric Processing of Nitrophenols and Nitrocresols From Biomass Burning Emissions, Journal of Geophysical Research: Atmospheres, 125, https://doi.org/10.1029/2020JD033401, 2020.
- Wang, J., Nie, W., Cheng, Y., Shen, Y., Chi, X., Wang, J., Huang, X., Xie, Y., Sun, P., Xu, Z., Qi, X., Su, H., and Ding, A.: Light absorption of brown carbon in eastern China based on 3-year multi-wavelength aerosol optical property observations and an improved absorption Ångström exponent segregation method, Atmos. Chem. Phys., 18, 9061–9074, https://doi.org/10.5194/acp-18-9061-2018, 2018a.
- Wang, L., Wang, X., Gu, R., Wang, H., Yao, L., Wen, L., Zhu, F., Wang, W., Xue, L., Yang, L., Lu, K., Chen, J., Wang, T., Zhang, Y., and Wang, W.: Observations of fine particulate nitrated phenols in four sites in northern China: concentrations, source apportionment, and secondary formation, Atmos. Chem. Phys., 18, 4349–4359, https://doi.org/10.5194/acp-18-4349-2018, 2018b.
- Wang, Y., Hu, M., Wang, Y., Zheng, J., Shang, D., Yang, Y., Liu, Y., Li, X., Tang, R., Zhu, W., Du, Z., Wu, Y., Guo, S., Wu, Z., Lou, S., Hallquist, M., and Yu, J. Z.: The formation of nitro-aromatic compounds under high NOx and anthropogenic VOC conditions in urban Beijing, China, Atmos. Chem. Phys., 19, 7649–7665, https://doi.org/10.5194/acp-19-7649-2019, 2019.
- Wang, Y., Jorga, S., and Abbatt, J.: Nitration of Phenols by Reaction with Aqueous Nitrite: A Pathway for the Formation of Atmospheric Brown Carbon, ACS Earth Space Chem., 7, 632–641, https://doi.org/10.1021/acsearthspacechem.2c00396, 2023.
- Wang, Z., Zhang, J., Zhang, L., Liang, Y., and Shi, Q.: Characterization of nitroaromatic compounds in atmospheric particulate matter from Beijing, Atmos. Environ., 246, https://doi.org/10.1016/j.atmosenv.2020.118046, 2021.
- Wang, Y., Huang, R.-J., Zhong, H., Wang, T., Yang, L., Yuan, W., Xu, W., and An, Z.: Predictions of the optical properties of brown

- carbon aerosol by machine learning with typical chromophores, Environ. Sci. Technol., 58, 20588–20597, 2024.
- Yang, J., Au, W. C., Law, H., Lam, C. H., and Nah, T.: Formation and evolution of brown carbon during aqueous-phase nitrate-mediated photooxidation of guaiacol and 5-nitroguaiacol, Atmos. Environ., 254, https://doi.org/10.1016/j.atmosenv.2021.118401, 2021.
- Yang, J., Au, W. C., Law, H., Leung, C. H., Lam, C. H., and Nah, T.: pH affects the aqueous-phase nitrate-mediated photooxidation of phenolic compounds: implications for brown carbon formation and evolution, Environmental Science: Processes & Impacts, 25, 176–189, https://doi.org/10.1039/D2EM00004K, 2023.